JOURNAL OF GEOPHYSICAL RESEARCH: ATMOSPHERES, VOL. 118, 7628–7639, doi:10.1002/jgrd.50571, 2013

Projection of occurrence of extreme dry-wet years and seasons in Europe with stationary and nonstationary Standardized Precipitation Indices

S. Russo,[1,2] A. Dosio,[1] A. Sterl,[3] P. Barbosa,[1] and J. Vogt[1]

Received 27 February 2013; revised 8 May 2013; accepted 12 June 2013; published 25 July 2013.

[1] The probabilities of the occurrence of extreme dry/wet years and seasons in Europe are estimated by using two ways of the Standardized Precipitation Index (SPI and SPI-GEV) and the Standardized Nonstationary Precipitation Index (SnsPI). The latter is defined as the SPI by fitting precipitation data with a nonstationary Gamma distribution in order to model the precipitation time dependence under climate change. Bias-corrected daily precipitation outputs from five different regional climate models (RCMs) provided by the ENSEMBLES project are used. The five RCMs are selected so as to represent the main statistical properties of the whole ENSEMBLES set and the most extreme deviation from the ensemble mean. All indicators are calculated for the ensemble of the five models over the period 1971–2098. Results show that under global warming, climate in Europe will significantly change from its current state with the probability of the occurrence of extreme dry and wet years and seasons increasing, respectively, over southern dry and northern wet regions. Comparing nonstationary and stationary indices, the SnsPI is found to be more robust than the common SPI in the prediction of precipitation changes with multimodel ensembles.

Citation: Russo, S., A. Dosio, A. Sterl, P. Barbosa, and J. Vogt (2013), Projection of occurrence of extreme dry-wet years and seasons in Europe with stationary and nonstationary Standardized Precipitation Indices, *J. Geophys. Res. Atmos.*, *118*, 7628–7639, doi:10.1002/jgrd.50571.

1. Introduction

[2] In the last few years, numerous extreme weather events, which have caused major human suffering and economic damage, have been recorded worldwide [*Comou and Rahmstorf*, 2012]. As an example, in the United States during the year 2011, new monthly heat records were broken for Texas, Oklahoma, and Delaware, whereas several northeastern states experienced the wettest winter on record [*Comou and Rahmstorf*, 2012].

[3] In Europe during the period 2000–2011, many wet and dry events were detected: For instance, autumn 2000 in England and Wales was the wettest since 1766 [*Alexander and Jones*, 2001], the largest daily rainfall of the past 100 years was recorded in Germany in 2002 [*Becker and Grünewald*, 2003], the wettest summer on record since 1901 occurred in Netherlands and Norway in 2011 [*World Meteorological Organization (WMO)*, 2011], and the summer of 2003 in southern Europe was the hottest of the last 500 years [*Luterbacher et al.*, 2004]. In particular, a very intense heat wave occurred in Spain. It was characterized by the persistence of very high temperatures, with 19 weather stations recording daily maximum temperatures equal to or higher than 40°C [*Barriopedro et al.*, 2011]. The impact of the heat wave in southern Europe was devastating: Mortality increased, especially in southwestern Europe, and an unusually large number of extensive forest fires occurred in Portugal, Spain, and France [*Díaz et al.*, 2005]. In 2007, the hottest summer on record since 1891 was recorded in Greece [*Founda and Giannakopoulos*, 2009], whereas in 2011, France experienced the hottest and driest spring since 1880 [*WMO*, 2011]. Many other extreme weather events happened in Europe in the last decade, as documented by, e.g., *Comou and Rahmstorf* [2012].

[4] All these events can be classified as "extremes." An extreme event is statistically defined as the occurrence of a value of a weather or climate variable above (or below) a threshold near the upper (or lower) end of the range of observed values [*Intergovernmental Panel on Climate Change* (*IPCC*), 2012]. Alternatively, a weather event can be considered extreme according to the amplitude of its impact on society and ecosystems [*IPCC*, 2012]. All the previous listed meteorological events fulfill both these conditions; they were rare and had a strong consequence on human health and ecosystems.

[1]Institute for Environment and Sustainability, Joint Research Centre, European Commission, Ispra, Italy.
[2]Institute for Environmental Protection and Research, Rome, Italy.
[3]Royal Netherlands Meteorological Institute, De Bilt, Netherlands.

Corresponding author: S. Russo, Institute for Environment and Sustainability, Joint Research Centre, European Commission, Via Enrico Fermi 2749, IT-21027, Ispra, Italy. (simone.russo@jrc.ec.europa.eu)

2169-897X/13/10.1002/jgrd.50571

[5] With the projected increase in temperature due to climate change, the question arises if these events will continue to be classified as "extremes" in the future. Many studies have assessed potential future changes in climate extremes, by showing that the 21st century will experience global changes in temperature and precipitation extremes consistent with a warming climate [*Alexander et al.*, 2006; *Kharin and Zwiers*, 2005; *Kharin et al.*, 2007; *Sterl et al.*, 2008; *Heinrich and Gobiet*, 2011; *Min et al.*, 2011; *Russo and Sterl*, 2012; *Avila et al.*, 2012; *Comou and Rahmstorf*, 2012; *Sillmann et al.*, 2013]. In these studies, different methods (e.g., Extreme Values Theory or Climate Indicators) have been used to project temperature and precipitation changes. In particular, *Heinrich and Gobiet* [2011] have computed a few drought indicators for diagnosing future drought occurrence in climate change scenarios. One of these indicators was the Standardized Precipitation Index (SPI) which is widely applied to characterize extreme dryness and wetness.

[6] In this study projections of dryness and wetness are estimated by means of the SPI and other precipitation indices, obtained as a modification of it. One of these indices is the SPI-GEV which is defined as the SPI but by modeling precipitation data with a generalized extreme value (GEV) distribution instead of a Gamma distribution. A second index is the Standardized Nonstationary Precipitation Index (SnsPI) using a nonstationary Gamma distribution in the modeling of the precipitation data. The SPI and SPI-GEV are classified here as stationary indices, whereas the SnsPI is classified as a nonstationary index. By computing the SPI, SPI-GEV, and SnsPI for daily precipitation outputs from five different regional climate models (RCMs) under the Special Report on Emissions Scenarios (SRES) A1B emission scenario provided by the ENSEMBLES project [*van der Linden and Mitchell*, 2009], we test whether these indices show any difference in the prediction of the probability of occurrence of extreme dry/wet years and seasons over Europe and investigate how this probability will change in a future changing climate.

2. Data

[7] In this work, we use outputs from high-resolution climate change projections performed by state-of-the-art global climate models (GCMs) and regional climate models (RCMs) in the framework of the Sixth Framework Programme project ENSEMBLES [*van der Linden and Mitchell*, 2009]. The aim of the ENSEMBLES project was to run multiple RCM-GCM simulations in order to improve the accuracy and reliability of climate models and to quantify and reduce the uncertainty in the climate projections [*van der Linden and Mitchell*, 2009]. The domain of the RCM simulations encompasses the whole of Europe at a resolution of about 25 km. The simulations cover the period 1961 and 2100 under the SRES A1B emission scenario.

[8] Bias correction of ENSEMBLES daily series of temperature and precipitation was performed by *Dosio and Paruolo* [2011] and *Dosio et al.* [2012], following the approach of *Piani et al.* [2010]. The bias correction was based on the E-OBS data set [*Haylock et al.*, 2008], a data set of daily observations of temperature and precipitation covering Europe for the period 1950–2008. The E-OBS data set has been evaluated and compared to other available data sets by, e.g., *Hofstra et al.* [2010]. As pointed out by *Dosio et al.* [2012], there may be some potentially important limitations to the data, such as inhomogeneities (both spatial and temporal) and large absolute and relative differences over regions where data sets developed with very dense station networks exist (e.g., British Isles). However, *Coppola et al.* [2010] claim that climate statistics for the E-OBS data set are very similar to, e.g., the Climatic Research Unit data set [*New et al.*, 2002].

Table 1. List of Bias-Corrected Model Runs Selected in This Study

Institute	RCM	Driving GCM
METO-HC	HadRM3Q0	HadCM3Q0
KNMI	RACMO2	ECHAM5r3
C4I	RCA3	HadCM3Q16
DMI	HIRHAM5	ARPEGE
DMI	HIRHAM5	ECHAM5

[9] *Dosio and Paruolo* [2011] showed that the bias correction improved significantly not only the present climate mean statistics but also the time-dependent properties, such as the number of consecutive dry days and the cumulative amount of rainfall for consecutive heavy precipitation days. The need for bias-correcting model projection is well known [e.g., *Christensen et al.*, 2008], and impact models may be significantly dependent on the occurrence and frequency of extreme events. For instance, *Rojas et al.* [2011] showed that the bias-corrected data significantly improve the simulation of river flood for the present climate.

[10] As process-based impact assessment models are often too expensive on time and resources to be run by using a large ensemble of climate runs as an input, *Dosio et al.* [2012] suggested that it is possible to select a subset of runs that represent both the main statistical properties of the whole ensemble (e.g., climate change signal) and the most extreme deviations from it, i.e., those that maximize the variability. The five bias-corrected ENSEMBLES runs selected for this study, shown in Table 1, have the following characteristics:

[11] 1. The KNMI-RACMO2-ECHAM5 run is the closest to the average of the whole ensembles.

[12] 2. The METO-HC HadRM3Q0-HadCM3Q0 shows a very warm and dry signal in summer, for both northern and southern Europe. In addition, it shows a warmer than average signal in winter, although slightly wetter.

[13] 3. The C4I RCA3-HadCM3Q16 is not only the warmest model in both winter and summer but also one of the wettest.

[14] 4. The DMI HIRHAM5-ARPEGE is always colder and drier than the average.

[15] 5. The DMI HIRHAM5-ECHAM5 shows a signal that is always colder and wetter than the average.

[16] It must be noted, however, that this selection is somewhat subjective, and other criteria, depending, for instance, on the indicator, study purpose, and area of interest, may lead to different subsets. All models are driven by the same emission scenario (SRES A1B), and thus, all runs represent an equally probable projection of the future evolution of the climate. However, the selected runs show a significant variability in the climate change signal for both temperature and precipitation [see *Dosio et al.*, 2012]. Specifically, the KNMI

Table 2. SPI Classification Following *McKee et al.* [1995]

SPI Values	Class	Probability of Event (%)
SPI > 2.00	Extreme wet	2.3
1.50 < SPI ≤ 2.00	Severe wet	4.4
1.00 < SPI ≤ 1.50	Moderate wet	9.2
–1.00 < SPI ≤ 1.00	Near normal	68.2
–1.50 < SPI ≤ –1.00	Moderate dry	9.2
–2.00 < SPI ≤ –1.50	Severe dry	4.4
SPI ≤ –2.00	Extreme dry	2.3

RACMO2-ECHAM5 run is the closest to the median of the five-model ensemble; the DMI HIRHAM5-ARPEGE shows a signal that is usually drier than the median of the five-model ensemble, whereas the DMI HIRHAM5-ECHAM5 predicts a wetter signal.

3. Precipitation Indices

3.1. The Standardized Precipitation Index

[17] The SPI is one of the most common and useful indicators for monitoring meteorological dry and wet periods. It is a precipitation-based index that was originally formulated by *McKee et al.* [1993]. The SPI can be estimated for different time scales by using precipitation amounts, from monthly up to yearly or even longer accumulation periods.

[18] In the classical SPI definition, precipitation amount records are fitted to a Gamma distribution. A Gamma-distributed variable X is continuous and positive and has a probability density function (PDF) defined by two parameters as follows:

$$f(x) = \frac{1}{s^a \Gamma(a)} x^{a-1} e^{-\frac{x}{s}}, \quad \text{for } x \geq 0 \text{ and } a, s > 0, \tag{1}$$

where s and a are, respectively, the scale and shape parameters and $\Gamma(a)$ is the mathematical Gamma function. The Gamma distribution with parameters s and a is denoted as Gamma(s, a). The expectation and variance of an $X \sim$ Gamma(s, a) variable are

$$E(X) = \mu = a \cdot s; \qquad \mathrm{Var}(X) = a \cdot s^2. \tag{2}$$

[19] The fitted distribution is then used to transform time series of annual or seasonal precipitation extremes into standard normal values. *McKee et al.* [1995] divided the standard normal values assumed by the SPI into moderate, severe, and extreme classes for both negative (dry) and positive (wet) SPIs (Table 2).

[20] This procedure is illustrated in Figure 1 for two points, one in southern Europe, close to Malaga, Spain (4.4°W, 36.86°N), and a second one in northern Europe near Stockholm, Sweden (15.84°E, 59.30°N). These two points have been selected because they experience different future changes, Malaga becoming drier and Stockholm becoming wetter. The black curves represent the CDFs fitted to the precipitation data of the reference period (1971–2000). The blue and brown curves are the corresponding fits for the future period (2069–2098). They will be discussed later. The CDF of the standard normal distribution is shown in green. A value of –2 for the standard normal distribution (green square in Figure 1) corresponds to a probability of 2.3% (y axis value × 100) that a year is extremely dry. By projecting this value onto the black curve, the corresponding precipitation amount is found (black square). For Malaga, this value is 230 mm/yr: There is a probability of 2.3% for any given year to have less than 230 mm of precipitation.

[21] The SPI is very flexible. Since it is a normalized measure relative to a specific location and period, it has the advantage that its values are climatologically consistent for any location. On the other hand, one of the disadvantages of the SPI as formulated by *McKee et al.* [1993] is that it cannot be used for a comparison between different time periods, which is required to assess the impact of climate change. In fact, since the SPI values are standardized (see Table 2) by using the Gamma distribution, they are specific to the period for which they are computed. Furthermore, as the SPI is based on the stationary Gamma distribution, it is not able to model time series longer than about 30 years; for longer time series, the climate change signal is expected to be significant; hence, the data cannot be treated as stationary and cannot be modeled with a stationary distribution.

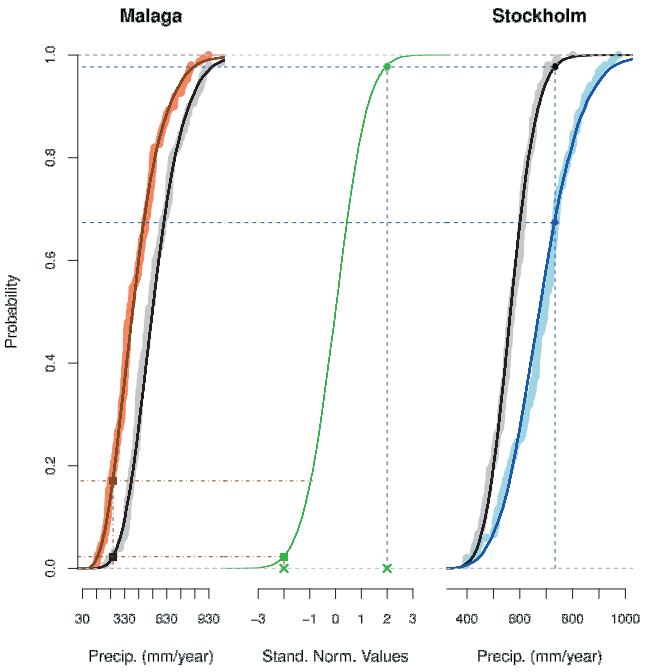

Figure 1. Relative SPI and SnsPI computation scheme. This example refers to the annual precipitation at two locations: one in southern Europe close to Malaga, Spain (4.4°W, 36.86°N), and a second one in northern Europe near Stockholm, Sweden (15.84°E, 59.30°N). The green curve is the standard normal CDF. The black curves represent the Gamma CDFs fitted to the yearly precipitation (gray filled circles) over the reference period (1971–2000) for the two selected locations. The blue and brown curves are the Gamma CDFs fitted to the precipitation data (light blue and orange) for a future period (2069–2098) for Stockholm and Malaga, respectively. The black filled circle (square) is the point for the present climate CDF corresponding to the SPI value 2 (green cross), which is the threshold of extreme wet (–2 for extreme dry; see Table 2). The blue filled circle (brown square) is the point representing the position of wet extreme today over the CDF fitted to the precipitation data for a future wetter (drier) period (2069–2098).

[22] To overcome these limitations, we proceed here in two different ways: first by using the SPI as a relative drought index [*Dubrovsky et al.*, 2009; *Heinrich and Gobiet*, 2011] (section 3.3) and then, as described in section 3.4, by adopting a new index which we call the Standardized Nonstationary Precipitation Index (SnsPI). By following the SnsPI definition (section 3.4), precipitation records are fitted by means of a nonstationary Gamma distribution. In this way, the SnsPI has the ability to model nonstationary time series, overcoming one of the limitations of the SPI, and therefore, it is expected to be more robust than the SPI in predicting precipitation changes.

3.2. The SPI-GEV Index

[23] There is some debate as to which parametric distribution should be selected for the accuracy of the final SPI values. *McKee et al.* [1995] have recommended the Gamma distribution, and *Lloyd-Hughes and Saunders* [2002] suggest that it is the most appropriate model for Europe. However, *Guttman* [1999] suggests that the Pearson-III distribution is the best universal model to adopt since its three parameters give it more flexibility than the Gamma distribution.

[24] In this study we do not go into this discussion; we just test if the SPI values are different if calculated with a three-parameter distribution rather than the Gamma distribution. Therefore, in addition to computing the SPI by means of a Gamma distribution, we modeled precipitation data using the generalized extreme values (GEV) distribution, defined by three parameters.

[25] The corresponding index is called SPI-GEV. The GEV distribution [*Coles*, 2001] is given by

$$G(x) = \exp\left\{-\left[1 + \xi\left(\frac{x-\mu}{\sigma}\right)\right]^{-1/\xi}\right\}. \quad (3)$$

The parameter μ describes the location of the distribution, the scale parameter σ its width, and the shape parameter ξ its asymmetry, determining the behavior of the tail. $G(x)$ is defined for $\{x : 1 + \xi\left(\frac{x-\mu}{\sigma}\right) > 0\}$, where the parameters satisfy $-\infty < \mu < +\infty$, $\sigma > 0$, and $-\infty < \xi < +\infty$. The cases $\xi = 0$, $\xi > 0$, and $\xi < 0$ define, respectively, the widely known Gumbel, Frechét, and Weibull distribution families.

3.3. The Relative SPI

[26] The relative SPI is defined with respect to a reference period, in our case 1971–2000 (current climate). To compute the relative SPI, the Gamma distribution is estimated for the reference and for the future period. The two curves are then used to calculate the probability difference between future and present SPI values. As an example, the blue and brown curves in Figure 1 are the CDFs fitted to the precipitation data of the future period (2069–2098), which is wetter (right shifting and widening of the PDF) in Stockholm and drier (left shifting of the PDF) in Malaga. For the present climate, we found a value of 230 mm/yr corresponding to a standard normal value of –2 (*extremely dry* according to Table 2) at Malaga. In the future climate (brown line), this same amount of rain corresponds to a probability of $\approx$ 18% (brown square) or, equivalently, to a standard normal value of $\approx$ –1 (near normal). The probability of an extreme dry year (according to present-day standards) has, therefore, increased sixfold. A similar procedure holds for the wet end of the distribution (circles in Figure 1). The relative SPI is computed in three different modes: with a Gamma distribution, with a GEV distribution, and by means of a GEV distribution with constant shape parameter for the reference and future periods. In the latter, the shape parameter of the GEV for the future period is imposed to be equal to the shape parameter of the GEV distribution fitted to the precipitation data over the reference period, and the resulting index is called SPI-GEV(ξ = const).

[27] In this study precipitation amounts are not transformed into standard normal values as in the classical SPI formulation but to probabilities (percentages) as described above and illustrated in Figure 1. The resulting probability SPI, ranging from 0 to 100%, is independent of grid points in different locations and climatic regions.

[28] A similar probability-based index was already introduced by *Min et al.* [2011] by fitting about 50 years of annual maxima of daily precipitation as well as 5 day consecutive precipitation amounts to a GEV distribution. In fitting the GEV distribution, *Min et al.* [2011] did not vary the GEV parameters with time but assumed that the location (μ), scale (σ), and shape (ξ) parameters are constant. However, in transient climate simulations, when the greenhouse forcing gradually changes, the assumption of stationarity is not necessarily valid [*Nikulin et al.*, 2011], since, over a period of 50 years, the climate change signal can be significant. In our case, since we use a 138 year time series of model-simulated annual and seasonal precipitation, the climate change signal is expected to be relevant; hence, we cannot treat the data as stationary. For a given grid point, the annual and seasonal precipitation are fitted to the Gamma distribution by varying the distribution parameters with time. This is done by computing the SnsPI, which is defined in the following section.

3.4. The SnsPI

[29] The SnsPI is defined like the relative SPI but using a nonstationary Gamma distribution to transform the precipitation time series into corresponding time series of probability values. The advantage of the SnsPI as compared to the SPI is that it is able to model the entire time series without splitting the data into shorter periods. Fitting precipitation data to a nonstationary model is done by linearly varying the scale parameter of the Gamma distribution with time. We thus assume that X_t (the precipitation amount in a future year t) can be modeled as

$$X_t \sim \text{Gamma}(s_t, a), \quad (4)$$

with $s_t = \mu_t/a$ and $E(X_t) = \mu_t = b_1 + b_2 t$, where b_1 and b_2 are constants.

[30] By doing so, variations through time are modeled by means of a Gamma distribution with different means and variances, but a common shape a. The rainfall data with a linear trend in the scale parameter as defined above are fitted by means of a regression model. A regression model for Gamma-distributed data is a generalized linear model fitted here by maximum likelihood [*McCullagh and Nelder*, 1989].

[31] The computation scheme is the same as that for the relative SPI. For the SnsPI, the CDF over a future period is obtained by means of the linear trend estimated in the

location parameter. As done for the SPI, we convert time series of seasonal and annual precipitation amounts into corresponding time series of probability values at each point of the model grid. This is done for the 138 year time series of each model and then for the ensemble of the five models fitted together by means of a covariate matrix [*McCullagh and Nelder*, 1989]. Comparison with SPI is done by estimating SnsPI probability values at the center of three selected 30 year periods (1971–2000, 2021–2050, and 2069–2098), which we denote as present, near future, and future, respectively.

4. Goodness of Fit and Significant Precipitation Changes

[32] Different goodness of fit tests are used depending on the stationarity or not of the time series. In the case of stationary time series, a Kolmogorov-Smirnov test (KS test) was carried out between precipitation data and the fitted Gamma and GEV distribution functions, respectively. The KS test is a popular goodness of fit statistic that measures the distance between the empirical distribution function and the specified distribution [*Von Storch and Zwiers*, 2003].

[33] In the case of the 138 year nonstationary time series (SnsPI), a statistic which is helpful to measure the goodness of fit of a given generalized linear model is the deviance defined as

$$D(y,\hat{\mu}) = 2\{l(y,y) - l(\hat{\mu},y)\}, \tag{5}$$

where $l(y,y)$ is the maximum likelihood achievable for an exact fit in which the fitted values are equal to the observed values and $l(\hat{\mu},y)$ is the log likelihood function calculated at the estimated parameters b_1, b_2, and a (see equation (4)). A small deviance implies a good fit. The null hypothesis has to be rejected at the α level of significance if $D > c_\alpha$, where c_α is the $(1-\alpha)$ quantile of the χ^2_k distribution [*Dobson*, 1990].

[34] The KS and deviance tests were also used to detect those grid points at which precipitation changes are *not* significant. In the case of stationary indices (SPI and SPI-GEV), the KS test is used to test whether precipitation in a future period is significantly different from that in the reference period. At each grid point, we test whether present and future amounts of rainfall are different, precisely, whether or not they are drawn from the same distribution at a chosen level of significance (5%).

[35] In order to detect grid points with nonsignificant precipitation changes according to the SnsPI, a log likelihood ratio test is used. The log likelihood ratio test uses the deviance (5) to verify if model Gamma(s,a) (M_0) is a subset of model Gamma(s_t,a) (M_1) [*McCullagh and Nelder*, 1989; *Coles*, 2001]. If $l_0(M_0)$ and $l_1(M_1)$ are, respectively, the maximized log likelihood for models M_0 and M_1, the deviance statistic can be calculated as

$$D = 2\{l_1(M_1) - l_0(M_0)\}. \tag{6}$$

A test of the validity of model M_0 relative to M_1 at the α level of significance is to reject M_0 in favor of M_1 if $D > c_\alpha$, where c_α is the $(1-\alpha)$ quantile of the χ^2_k distribution.

5. Results

5.1. Empirical Evaluation of Model Outputs

[36] Figure 2 shows the differences between future climate (2069–2098) and current climate (1971–2000) of the 2nd (extreme dry) and the 98th (extreme wet) percentile of the annual precipitation amounts. Results are shown for each model output separately and for the set of five-model ensemble simulations together; the latter is a set of 150 (5 models $\times$ 30 years) precipitation events, defined as follows:

$$E_5 = \bigcup_{m=1}^{5} \bigcup_{y=y_{\min}}^{y_{\max}} P_{m,y}, \tag{7}$$

with $(y_{\min}, y_{\max}) = (1971, 2000)$ and $(y_{\min}, y_{\max}) = (2069, 2098)$, respectively, for current and future climate. Here $\cup$ denotes the union of sets, m is the model of the five ensemble members, and $P_{m,y}$ is the total precipitation of model m in year y.

[37] Generally, each model simulates a wetter future climate over northern Europe and a drier one over southern Europe. However, differences exist between the models. Between northern Europe, where the climate is becoming wetter, and southern Europe, where it is becoming dryer, there exists a zonal band for which projections of 21st century precipitation change are very uncertain. Some models predict a significantly wetter climate, whereas others predict a drier one. This uncertainty may have a large impact when the whole ensemble of model data is used. In fact, the climate change signal can vary with the type of estimator used to make predictions. As an example, the 2nd and 98th percentiles of the five-member ensemble annual precipitation have been estimated here for the current and future periods in two different ways: as the percentiles of the set E_5 (see equation (7)) (Estim-1) and as the median of the five 2nd and 98th percentiles calculated for each single model (Estim-2). Differences between future and current Estim-1 and Estim-2 values (Figure 2) show an opposite behavior in the transition region between northern Europe and southern Europe. In the band stretching from Great Britain via southern Germany to the Carpathian Mountains, Estim-1 is negative, indicating drying, while Estim-2 is positive, indicating wettening.

[38] In the first case, the dry signal is due to the fact that the weighting given to each model is not equal. In fact, by considering a set of data built by the totality of the five models, the upper and lower extreme precipitation values of the sorted data are those of the wettest and driest models, respectively. For example, although three models predict a wetter climate in the future and two a drier one, the future-past difference of Estim-1 may result in a negative number, indicating that the future climate is becoming drier, even if we have a larger number of models predicting a wetter climate.

[39] In the second case, by estimating first the 2nd and 98th percentiles for each single model and then computing the median, the same weight is given to each model, meaning that if three of the models are drier and two are wetter, the future climate will be drier. This discrepancy will also be evident when the SPI is compared to the SnsPI, as discussed below. In the following section, by using SPI and SnsPI values expressed as probability (see section 3), it will be shown that the SPI is more representative of Estim-1, whereas

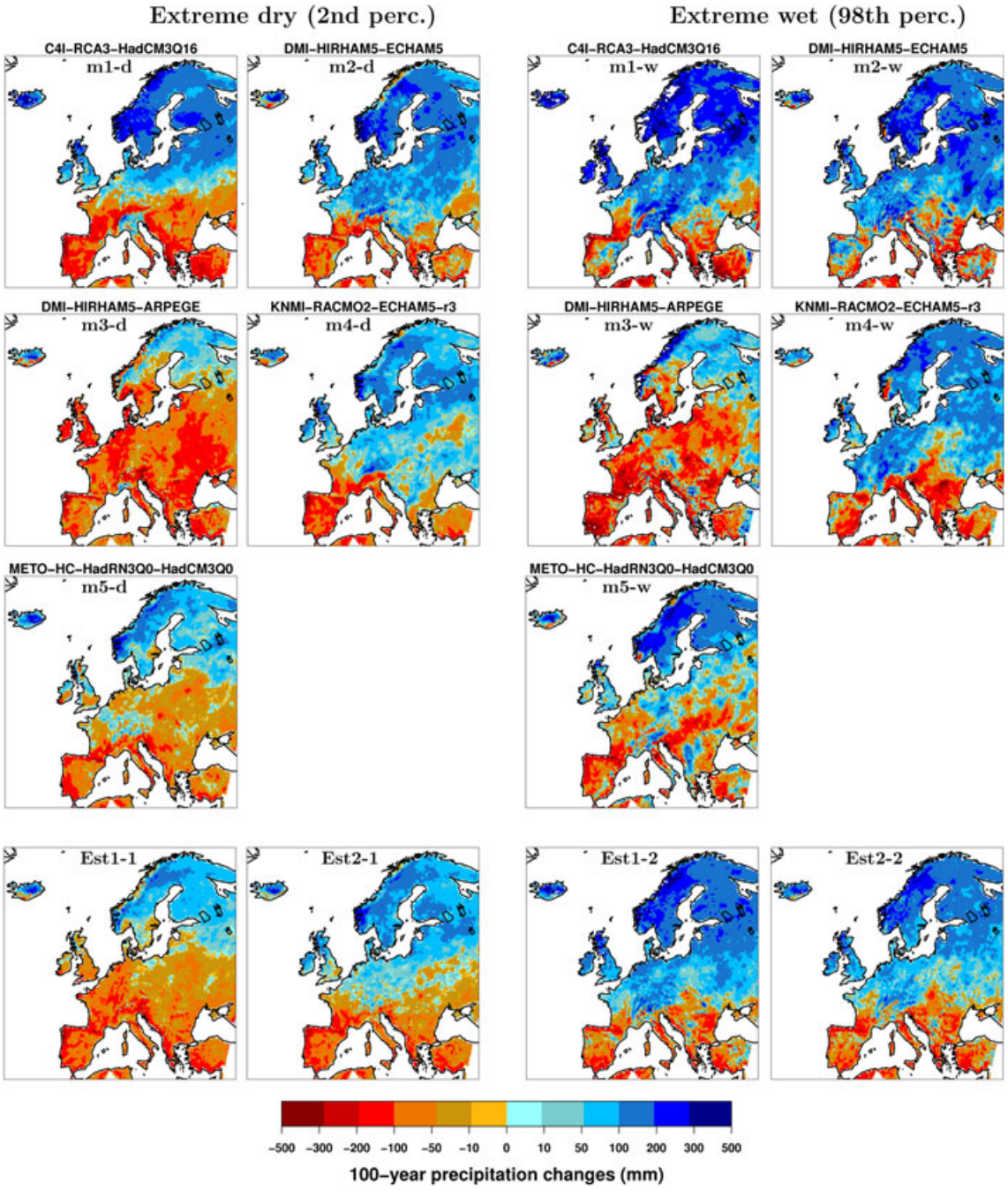

Figure 2. Differences between future climate (2069–2098) and current climate (1971–2000) of the 2nd and the 98th percentile of the annual precipitation amounts for each model data (m1-d to m5-d and m1-w to m5-w) and for the whole five-model ensemble by means of Estim-1 (Est1-1 and Est1-2) and Estim-2 (Est2-1 and Est2-2) as defined in section 5.1.

the SnsPI resembles Estim-2, giving equal weight to each single model.

5.2. Description of the Results

5.2.1. General Considerations

[40] Figures 3–5 show near-future (Figures 3a1–3c1, 3a3–3c3, 4a1–4c1, 4a3–4c3, 5a1–5c1, and 5a3–5c3) and future (Figures 3a2–3d2, 3a4–3d4, 4a2–4d2, 4a4–4d4, 5a2–5d2, and 5a4–5d4) changes of the occurrence of extreme dry/wet years and seasons (December–February (DJF) and June–August (JJA)), measured by means of the stationary and nonstationary SPIs (expressed as probability), computed for the whole ensemble of data as defined in equation (7). The period 1971–2000 (present) is used as the reference to measure future probability changes of precipitation amounts. The changes are calculated for two time windows of 30 years: 2021–2050 (near future) and 2069–2098 (future), with respect to the reference period. The significance of the probability differences between future and present periods for nonstationary (SnsPI) and stationary (SPI and SPI-GEV)

indices is evaluated, respectively, by means of a likelihood ratio test and a KS test (see section 4). In Figures 3–5, areas where, according to the used hypothesis tests at the chosen significance level of 5%, future precipitation amounts are not different from the present are masked out in white.

[41] The color scale ticks in Figures 3–5 are chosen according to the probability values reported in Table 2 in order to detect if, in the future, SPI probability values are moving into a different SPI level than the present. For instance, an SPI probability changing by more than 15.9%, i.e., the sum of the extreme (2.3%), severe (4.4%), and moderate (9.2%) SPI probability levels (see Table 2), means that precipitation amounts that are extreme in the current climate will be normal in the future.

5.2.2. Near-Future Extreme Year

[42] Near-future SPI and SPI-GEV extreme dry year changes are found to be significant for only a small portion of Europe (Figures 3b1 and 3c1), mainly in northern Spain, Portugal, and the Mediterranean areas (southern Spain, Greece, southern Italy, and southern Turkey), in agreement with *Heinrich and Gobiet* [2011]. Both indicators predict equal patterns and values of probability changes. The SnsPI shows a larger area, covering central Spain and southwestern France, with significant probability changes in the near future (Figure 3a1).

[43] The SnsPI maximum probability changes are found in southwestern France, with values exceeding 6.7%, meaning that a present extreme dry year will be normally dry in the near future.

[44] The probability of having an extreme wet year in the period 2021–2050 is increasing almost everywhere over northern Europe (Figures 3a3–3c3). All indicators (SPI, SPI-GEV, and SnsPI) show approximately the same patterns with equal probability difference values. The largest changes in the occurrence of extreme wet years are found over Scandinavia. In some parts of this region, a present extreme wet year is expected to become a normal event according to the SnsPI values. The probability is projected to increase by more than 15.9%.

5.2.3. Future Extreme Year

[45] At the end of the century (Figures 3a2–3c2 and 3a4–3c4), the area where significant SPI and SPI-GEV changes are projected is more extended as compared to the period 2021–2050. The regions where probability changes of occurrence of an extreme year are statistically insignificant (white area) are the same for both SnsPI and SPI. They form a narrow band over central Europe, stretching from northern France eastward to the northern coast of the Black Sea.

[46] This result is robust since two different statistical methods (KS test and log likelihood ratio test, respectively, for stationary and nonstationary indices) give the same result for the significance of the precipitation changes. It has to be noted, however, that the insignificance of the annual signal may be due to opposing seasonal signals. For instance, wetter winters and dryer summers in the future may result in an insignificant annual change.

[47] From the analysis of Figures 3a2–3c2, we note a zonal band between roughly 40°N and 60°N where the stationary (SPI and SPI-GEV) and nonstationary (SnsPI) indicators give opposite results. This opposite behavior could be associated with different values of the shape parameter of the fitted distributions. When the nonstationary Gamma distribution is used, the shape parameter does not vary with time, while for the stationary Gamma and GEV model, the shape parameter may differ between present climate and future climate. To test if the shape parameter estimated for annual rainfall has invariant properties with time and if a constant future shape parameter will give different estimates for the stationary indicators, we have introduced a new stationary index called SPI-GEV(xi=const). It is defined as the SPI-GEV by imposing the same shape parameter for both the present and future GEV distributions.

[48] Probability differences estimated with the SPI-GEV(xi=const) index are shown in Figures 3d2 and 3d4. We see that apart from some isolated locations, in the entire studied domain, the SPI-GEV(xi=const) values are reproducing the same patterns as the SPI and SPI-GEV stationary indicators. In particular, the SPI-GEV(xi=const) yields the same future drier signal in the band between 40°N and 60°N as the SPI, which is opposite to the SnsPI wetter trend in the same region.

[49] This yields two important results: The first is that for 12 month precipitation amounts, we can assume that the shape parameter is not significantly changing under climate change. This is an addition to that by *Wilson and Toumi* [2005], who have demonstrated that the shape parameter has invariant properties for daily rainfall. Furthermore, the different behavior between stationary and nonstationary indicators does not depend on shape but only on scale. This observation justifies the choice to make only the scale parameter time dependent in (4). We conclude that the SnsPI is more robust than the SPI in the detection of extreme wet and dry periods.

[50] While, over all parts of southern Europe, extreme dry events are more common in the future, the probability to have an extreme dry year in northern Europe is slightly decreasing by values not exceeding 2.3%. All indicators show the same pattern. In the south, a very dry pattern is detected with many locations affected by very high changes with values exceeding the level of normality by more than 15.9%. The current extreme events will become normal in the future over many southern European regions.

5.2.4. Changes During Summer (JJA) and Winter (DJF) Seasons

[51] Figures 4 and 5 show near-future (Figures 4a1–4c1, 4a3–4c3, 5a1–5c1, and 5a3–5c3) and future (Figures 4a2–4d2, 4a4–4d4, 5a2–5d2, and 5a4–5d4) probability changes of occurrence of extreme dry and wet seasons, estimated by means of the stationary and nonstationary indicators.

5.2.4.1. Summer Season

[52] From Figure 4, we note that when using the SPI and SPI-GEV (Figures 4b1 and 4c1), only a very small area (less than 5% of Europe) is expected to become drier in the middle of the 21st century. In contrast, the SnsPI values (Figure 4a1) exhibit a different pattern. The probability of extreme dry events increases over approximately 20% of the European region.

[53] For the future period, the discrepancy between the stationary and nonstationary indices in predicting extreme dry precipitation changes is even more evident (Figures 4a2–4d2). While both stationary and nonstationary indices predict the same patterns (dryer in the south and wetter in the north), the predicted probability for the occurrence of a future extreme dry summer is overestimated by the

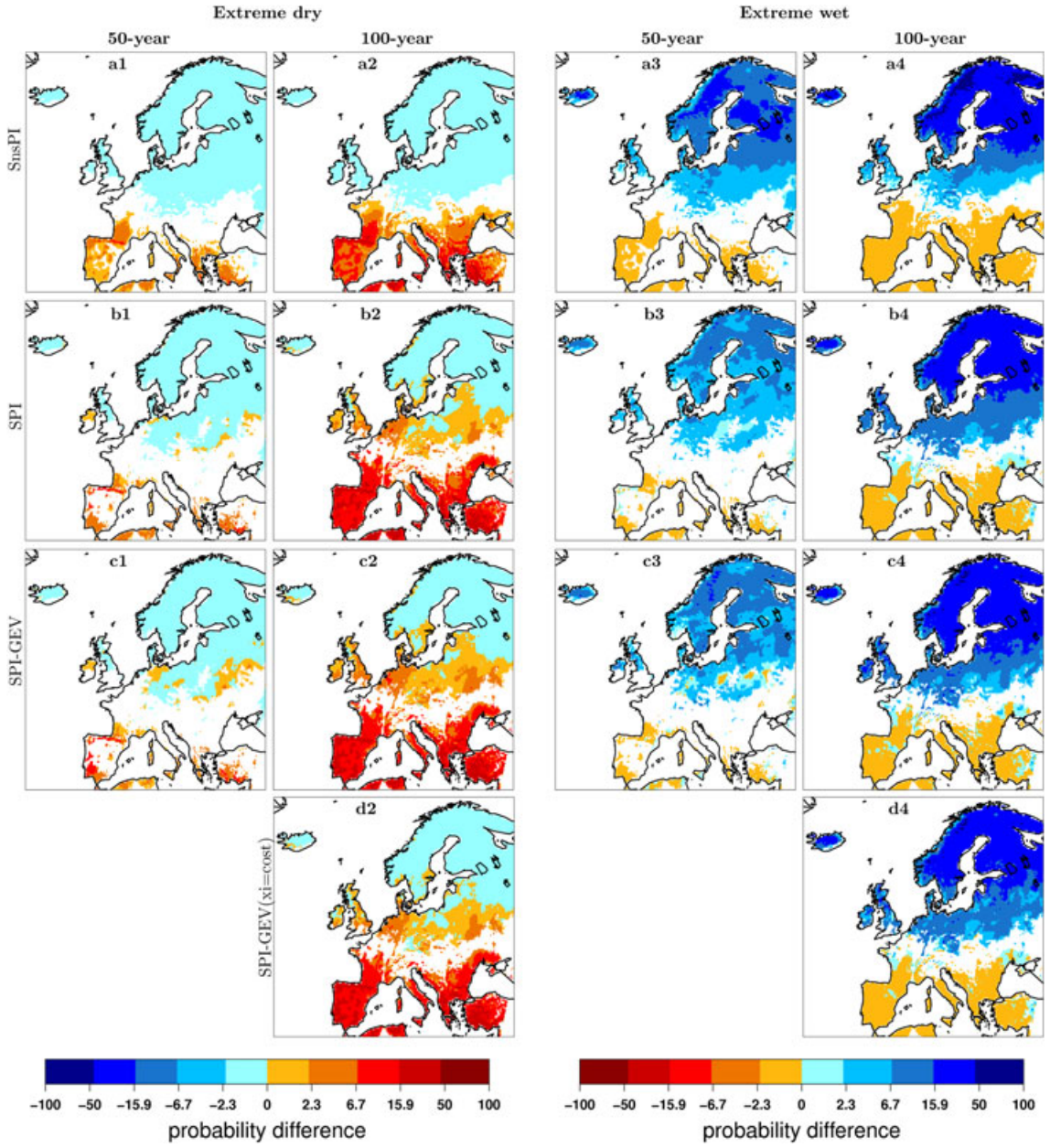

Figure 3. Probability changes over 50 and 100 years for extreme (a1–c1 and a2–d2) dry and (a3–c3 and a4–d4) wet years. The white areas represent the points where precipitation changes are not statistically significant at the 5% level according to the results of the log likelihood ratio test in Figures 3a1–3a4 or the KS test in Figures 3b1–3b4, 3c1–3c4, 3d2, and 3d4.

stationary indices with respect to the SnsPI. This overestimation is particularly evident over central Europe, where the SPI changes are in a higher probability class than the SnsPI. For example, in Brittany (northwestern France), the SPI-estimated probability changes are in the normal probability class (between 15.9% and 50%), while the SnsPI gives values in the moderate class (between 6.7% and 15.9%).

[54] The results of the nonstationary index are found to be more robust, as the SnsPI estimation is performed by using a longer sample of data (138 years × 5 members) than the stationary indices (time period of 30 years × 5 members). The SPI projections are obtained by taking only the first (1971–2000) and the last 30 years (2069–2098) of the data sample and ignoring the rest. For each of these periods, one value of the distribution parameters is calculated, so that the calculated change is effectively based on the difference between two periods, and any nonlinear dependence on time is disregarded. The climate change signal is better represented by the SnsPI, which takes all data into account.

[55] According to the SnsPI results (Figures 4a1 and 4a2), southern Europe is getting drier, especially over northern Portugal, Spain, France, and the Mediterranean region. This is consistent with earlier results [e.g., *Intergovernmental Panel on Climate Change*, 2007; *Quesada et al.*, 2012]. In some areas of these regions, the probability of occurrence of an extreme dry summer increases by more than

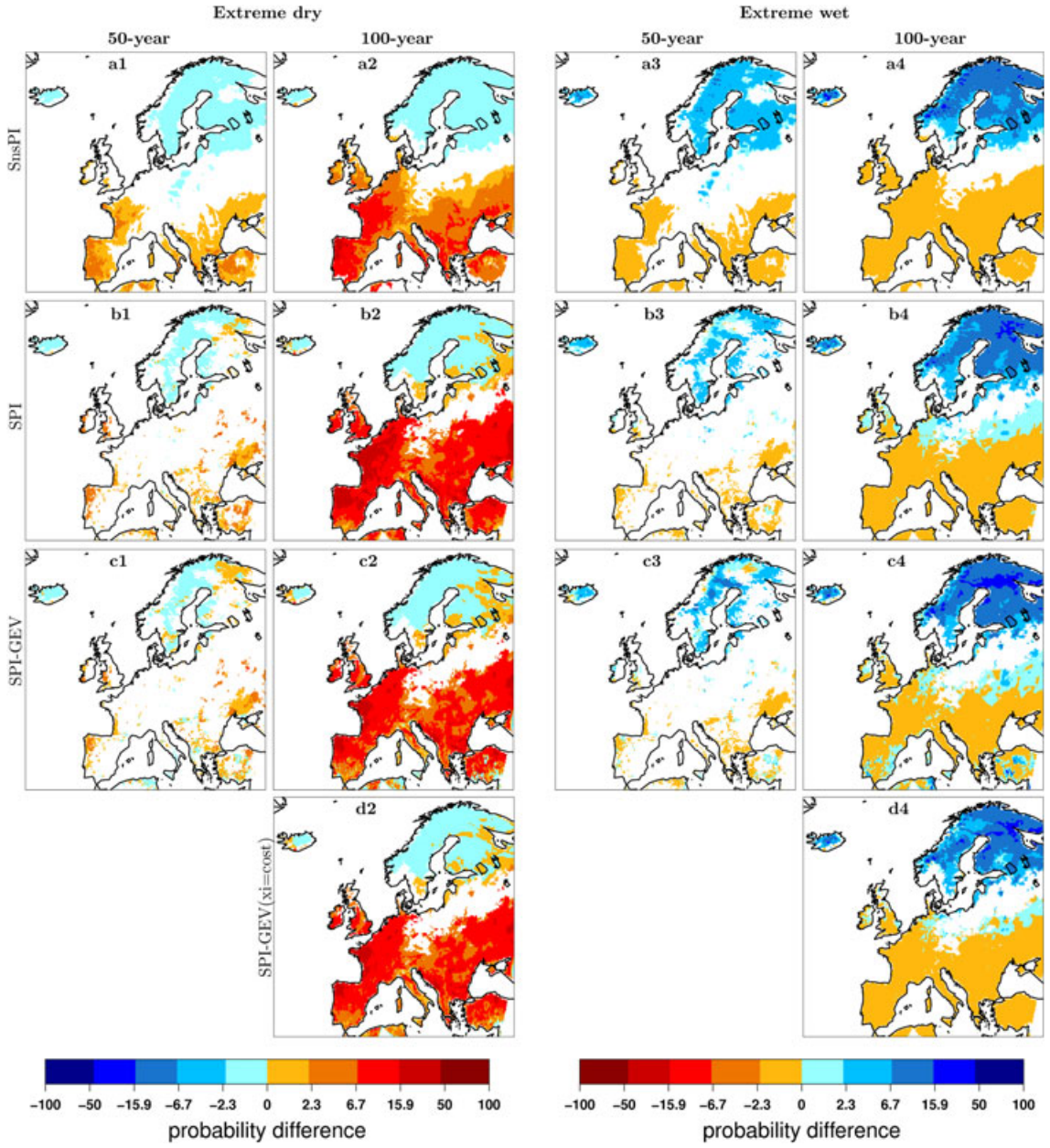

Figure 4. As in Figure 3 but for the summer season (JJA).

2.3% and 6.7% in the near future and future, respectively. This indicates that what is currently an extreme dry summer will become a severely dry one in the middle of the 21st century and a moderate one at the end of the century. In the latter period, the band with an increasing occurrence of extreme dry summer seasons is zonally moving by about 10° farther southward than for the whole year (Figure 3a2). The dry European areas will become even drier in summer (JJA) and may also expand northward, including the region of central Europe where no climate change signal was detected on the annual scale. Probability decreases occur mainly in the Scandinavian regions with SnsPI probability difference values smaller than 2.3% (Figures 4a1 and 4a2), meaning that the extreme dry summer season will become wetter in the near future but still remain in the extreme dry probability class.

[56] The probability of occurrence of an extreme wet summer (Figures 4a3–4c3 and 4a4–4d4) shows the same pattern as for the extreme dry summer: dryer in the south and wetter in the north. However, in this case, the wettening in the north is more intense than the drying detected in the south. The wet signal exceeds the value of 6.7% over many locations in Scandinavia, according to all (stationary and nonstationary) indices. In the future, an extreme wet summer will occur more frequently over northern Europe.

5.2.4.2. Winter Season

[57] As shown in Figure 5, all indices used agree in the projection of extreme dry and wet winters. For all indices, the projections are the same in terms of estimated values and regions where near-future and future winters are expected to become dryer or wetter.

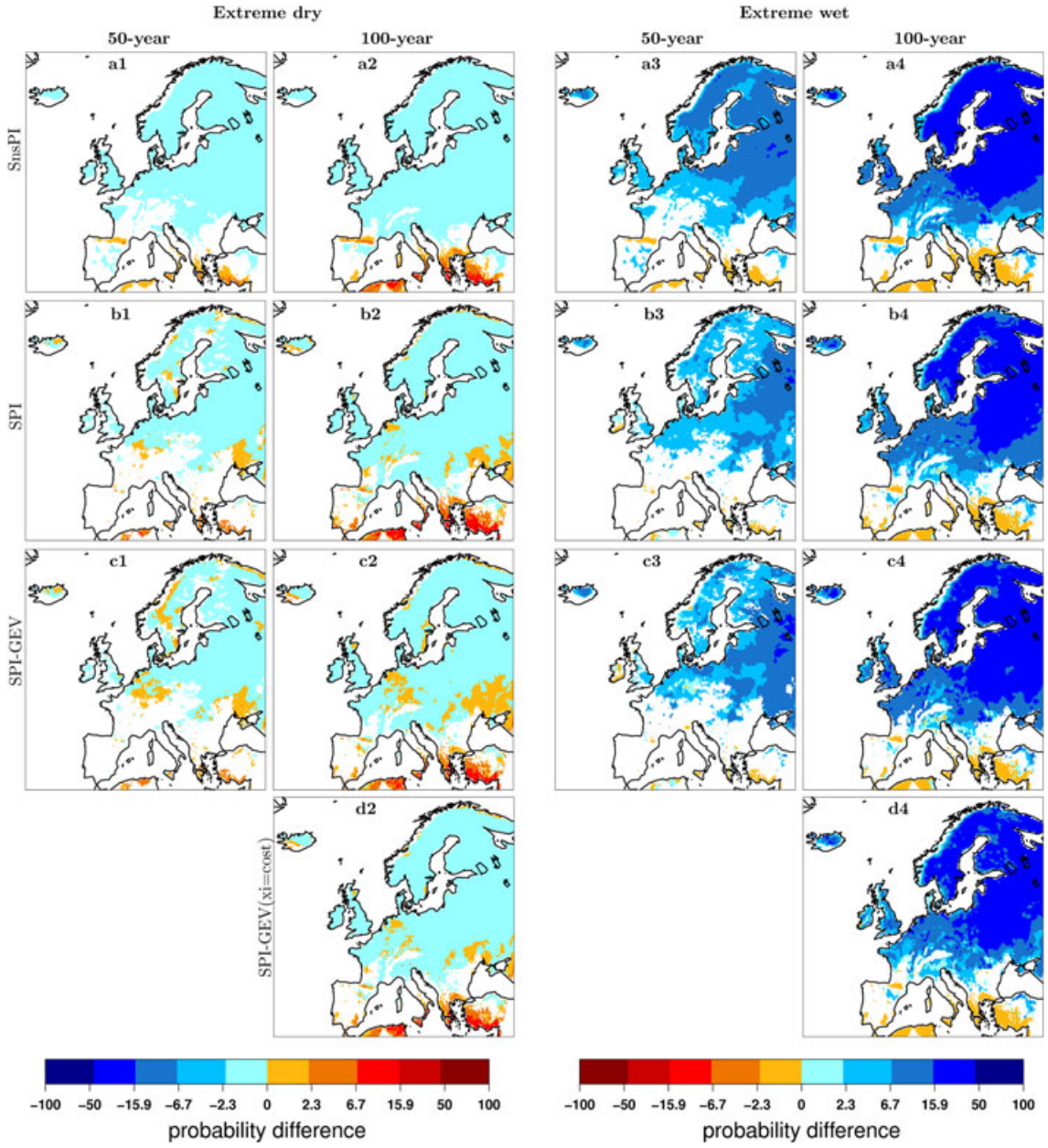

Figure 5. As in Figure 3 but for the winter season (DJF).

[58] In most parts of central and northern Europe, extreme dry winter seasons show a small wetting signal, with values not exceeding 2.3% (Figures 5a1–5c1 and 5a2–5d2) for both the near-future and future periods. In southern Europe, changes are mainly insignificant. The exceptions are some Mediterranean regions such as Greece, southern Italy, and Turkey, where the winter season is expected to be drier than that in the present period. This could lead to severe consequences for water management and, consequently, affect agriculture [*Hisdal et al.*, 2001]. Furthermore, in these regions, also the probability of occurrence of an extreme wet winter (Figures 5a3–5c3 and 5a4–5d4) slightly decreases.

[59] The probability of occurrence of an extreme wet winter in the near future and future, according to all indices, increases in central and northern Europe (Figures 5a3–5c3 and 5a4–5d4). The area showing a wettening signal is larger for the future than for the near-future period, and the probability increases. The largest changes are found in Russia and Scandinavia, where the probability differences reach values around 20% for all indices. As a consequence, present wet-extreme winters will become normal in the future.

[60] As for the summer dry season, the SnsPI indicates that the band with an increasing occurrence of extreme wet winter seasons is zonally moving by about 10° farther southward than for the whole year (Figure 4a4). Wet European areas will become even wetter in winter and expand southward. This includes the central European region which is becoming drier in summer and wetter in winter, but shows a nonsignificant change for annual rainfall amounts.

6. Discussion and Conclusion

[61] In this study standardized stationary and nonstationary precipitation indices (SPI, SPI-GEV, and SnsPI) have

been used to estimate future changes of the probability of occurrence of extreme dry/wet seasons and years in Europe. The indices were calculated by using daily precipitation data from a five-member model ensemble, under the A1B emission scenario. The model outputs were bias corrected according to *Dosio and Paruolo* [2011] and *Dosio et al.* [2012], following the approach of *Piani et al.* [2010]. Precipitation, and especially heavy precipitation, is strongly dependent on details of the climate models parametrization [e.g., *Emori et al.*, 2005], and the use of a bias-corrected multimodel ensemble gives more robust results in the prediction of climate change.

[62] The SnsPI is found to be more robust in describing precipitation changes as it uses data over the whole period (here 1971–2098) rather than from two subperiods only, as for the SPI.

[63] Summarizing our results, we find that under the A1B climate change scenario, the probability of having an extreme precipitation season is increasing over all of Europe, with wet and dry regions becoming, respectively, wetter and drier. The signal is more pronounced for seasonal (winter and summer) than for annual values because of compensating effects. Today's extreme dry and wet seasons will become, respectively, dryer and wetter within the next 100 years. From a statistical point of view, these changes are mainly associated with the shifting and widening of the location and scale parameters, while the shape parameter does not change significantly neither for annual nor for seasonal precipitation amounts.

[64] In all seasons, the probability to have an extreme wet (dry) period is increasing northward (southward) and decreasing southward (northward) of central Europe, where changes are small. The position of the boundary between areas becoming drier/wetter moves zonally by about 10° during the annual cycle.

[65] The magnitude of the probability changes for extreme precipitation increases with time. Maximum wet (dry) changes are found in winter (summer) in northern (southern) Europe. Throughout the simulation period, the spatial patterns of change are the same with dry areas becoming drier and wet areas becoming wetter.

[66] **Acknowledgments.** The authors thank Andrew Singleton for the useful discussions. The ENSEMBLES data used in this work were funded by the EU-FP6 integrated project ENSEMBLES (contract 505539; http://ensembles-eu.org) whose support is gratefully acknowledged. We thank the anonymous reviewers, whose critical comments helped to considerably improve the paper.

References

Alexander, L. V., and P. D. Jones (2001), Updated precipitation series for UK and discussion of recent extremes, *Atmos. Sci. Lett.*, *1*, 1–9.

Alexander, L. V., et al. (2006), Global observed changes in daily climate extremes of temperature and precipitation, *J. Geophys. Res.*, *111*, D05109, doi:10.1029/2005JD006290.

Avila, F. B., A. J. Pitman, M. G. Donat, L. V. Alexander, and G. Abramowitz (2012), Climate model simulated changes in temperature extremes due to land cover change, *J. Geophys. Res.*, *117*, D04108, doi:10.1029/2011JD016382.

Barriopedro, D., E. M. Fischer, J. Luterbacher, R. M. Trigo, and R. Garca-Herrera (2011), The hot summer of 2010: Redrawing the temperature record map of Europe, *Science*, *332*, 220–224, doi:10.1126/science.1201224.

Becker, A., and U. Grünewald (2003), Flood risk in central Europe, *Science*, *300*, 1099.

Christensen, J. H., F. Boberg, O. B. Christensen, and P. Lucas Picher (2008), On the need for bias correction of regional climate change projections of temperature and precipitation, *Geophys. Res. Lett.*, *35*, L20709, doi:10.1029/2008GL035694.

Coles, S. (2001), *An Introduction to Statistical Modeling of Extreme Values*, 208 pp., Springer-Verlag, Berlin.

Comou, D., and S. Rahmstorf (2012), A decade of weather extremes, *Nat. Clim. Change*, *2*, 491–496, doi:10.1038/NCLIMATE1452.

Coppola, E., F. Giorgi, S. A. Rausher, and C. Piani (2010), Model weighting based on mesoscale structures in precipitation and temperature in an ensemble of regional climate models, *Clim. Res.*, *44*, 121–134, doi:10.3354/cr00940.

Díaz, J., R. García-Herrera, R. M. Trigo, C. Linares, M. A. Valente, J. M. De Miguel, and E. Hernández (2005), The impact of the summer 2003 heat wave in Iberia: How should we measure it? *Int. J. Biometeorol.*, *50*, 159–66, doi:10.1007/s00484-005-0005-8.

Dobson, A. (1990), *An Introduction to Generalized Linear Models,* 2nd ed., CRC Press, Boca Raton, FL.

Dosio, A., P. Paruolo, and R. Rojas (2012), Bias correction of the ENSEMBLES high resolution climate change projections for use by impact models: Analysis of the climate change signal, *J. Geophys. Res.*, *117*, D17110, doi:10.1029/2012JD017968.

Dosio, A., and P. Paruolo (2011), Bias correction of the ENSEMBLES high-resolution climate change projections for use by impact models: Evaluation on the present climate, *J. Geophys. Res.*, *116*, D16106, doi:10.1029/2011JD015934.

Dubrovsky, M., M. D. Svoboda, M. Trnka, M. J. Hayes, D. A. Wilhite, Z. Zalud, and P. Hlavinka (2009), Application of relative drought indices in assessing climate-change impacts on drought conditions in Czechia, *Theor. Appl. Climatol.*, *96*, 155–171.

Emori, S., A. Hasegawa, T. Suzuki, and K. Dairaku (2005), Validation, parameterization dependence, and future projection of daily precipitation simulated with a high-resolution atmospheric GCM, *Geophys. Res. Lett.*, *32*, L06708, doi:10.1029/2004GL022306.

Founda, D., and C. Giannakopoulos (2009), The exceptionally hot summer of 2007 in Athens, Greece. A typical summer in the future climate? *Global Planet. Change*, *67*, 227–236.

Guttman, N. B. (1999), Accepting the Standardized Precipitation Index: A calculation algorithm, *J. Am. Water Resour. Assoc.*, *35*, 311–322.

Haylock, M. R., N. Hofstra, A. M. G. Klein Tank, E. J. Klok, P. D. Jones, and M. New (2008), A European daily high-resolution gridded data set of surface temperature and precipitation for 1950–2006, *J. Geophys.Res.*, *113*, D20119, doi:10.1029/2008JD010201.

Heinrich, G., and A. Gobiet (2011), The future of dry and wet spells in Europe: A comprehensive study based on the ENSEMBLES regional climate models, *Int. J. Climatol.*, *32*, 1951–1970, doi:10.1002/joc.2421.

Hisdal, H., K. Stahl, L. M. Tallaksen, and S. Demuth (2001), Have streamflow droughts in Europe become more severe or frequent? *Int. J. Climatol.*, *21*, 317–333, doi:10.1002/joc.619.

Hofstra, N., M. New, and C. McSweeney (2010), The influence of interpolation and station network density on the distribution and extreme trends of climate variables in gridded data, *Clim. Dyn.*, *35*, 841–858, doi:10.1007/s00382-009-0698-1.

Intergovernmental Panel on Climate Change (2007), *Climate Change 2007, The Physical Science Basis. Contribution of Working Group I to the Fourth Assessment Report on the Intergovernmental Panel on Climate Change*, 996 pp. S. Solomon et al. (eds), Cambridge Univ. Press, Cambridge, U. K.

Intergovernmental Panel on Climate Change (IPCC) (2012), *Managing the Risks of Extreme Events and Disasters to Advance Climate Change Adaptation. A Special Report of Working Groups I and II of the Intergovernmental Panel on Climate Change*, 582 pp. C. B. Field et al. (eds), Cambridge Univ. Press, Cambridge, U. K.

Kharin, V. V., and F. W. Zwiers (2005), Estimating extremes in transient climate change simulations, *J. Clim.*, *18*, 1156–1173.

Kharin, V. V., F. W. Zwiers, X. Zhang, and G. C. Hegerl (2007), Changes in temperature and precipitation extremes in the IPCC ensemble of global coupled model simulations, *J. Clim.*, *20*, 1419–1444, doi:10.1175/JCLI4066.1.

Lloyd-Hughes, B., and M. A. Saunders (2002), A drought climatology for Europe, *Int. J. Climatol.*, *22*, 1571–1592.

Luterbacher, J., D. Dietrich, E. Xoplaki, M. Grosjean, and H. Wanner (2004), European seasonal and annual temperature variability, trends, and extremes since 1500, *Science*, *303*, 1499–1503.

McCullagh, P., and J. A. Nelder (1989), *Generalized Linear Models*, 511 pp., Chapman and Hall, London.

McKee, T. B., N. J. Doesken, and J. Kleist (1993), The relationship of drought frequency and duration to time scales, *paper presented at 8th Conference on Applied Climatology, Am. Meteorol. Soc., Anaheim, Calif.*

McKee, T. B., N. J. Doesken, and J. Kleist (1995), Drought monitoring with multiple time scales, *paper presented at 9th Conference on Applied Climatology, Am. Meteorol. Soc., Dallas, Tex.*

Min, S., X. Zhang, F. W. Zwiers, and G. C. Hegerl (2011), Human contribution to more-intense precipitation extremes, *Nature*, *470*, 378–381, doi:10.1038/nature09763.

New, M., D. Lister, M. Hulme, and I. Makin (2002), A high-resolution data set of surface climate over global land areas, *Clim. Res.*, *21*, 1–25, doi:10.3354/cr021001.

Nikulin, G., E. Kjellström, U. Hansson, C. Jones, G. Strandberg, and A. Ullerstig (2011), Evaluation and future projections of temperature, precipitation and wind extremes over Europe in an ensemble of regional climate simulations, *Tellus, Ser. A*, *63*, 41–55, doi:10.1111/j.1600-0870.2010.00466.x.

Piani, C., J. O. Haerter, and E. Coppola (2010), Statistical bias correction for daily precipitation in regional climate models over Europe, *Theor. Appl. Climatol.*, *99*, 187–192, doi:10.1007/s00704-009-0134-9.

Quesada, B., R. Vautard, P. Yiou, M. Hirschi, and S. I. Seneviratne (2012), Asymmetric European summer heat predictability from wet and dry southern winters and springs, *Nat. Clim. Change*, *2*, 736–741, doi:10.1038/NCLIMATE1536.

Rojas, R., L. Feyen, A. Dosio, and D. Bavera (2011), Improving pan-European hydrological simulation of extreme events through statistical bias correction of RCM-driven climate simulations, *Hydrol. Earth Syst. Sci.*, *15*, 2599–2620, doi:10.5194/hess-15-2599-2011.

Russo, S., and A. Sterl (2012), Global changes in seasonal means and extremes of precipitation from daily climate model data, *J. Geophys. Res.*, *117*, D01108, doi:10.1029/2011JD016260.

Sillmann, J., V. V. Kharin, F. W. Zwiers, X. Zhang, and D. R. Bronaugh (2013), Climate extreme indices in the CMIP5 multi-model ensemble. Part 2: Future climate projections, *J. Geophys. Res. Atmos.*, *118*, 1716–1733, doi:10.1002/jgrd.50203.

Sterl, A., C. Severijns, W. Hazeleger, G. Burgers, B. van den Hurk, G. J. van Oldenborgh, P. van Velthoven, H. Dijkstra, P. J. van Leeuwen, and M. van den Broeke (2008), When can we expect extremely high surface temperatures? *Geophys. Res. Lett.*, *35*, L14703, doi:10.1029/2008GL034071.

van der Linden, P., and J. F. B. Mitchell (2009), *ENSEMBLES: Climate change and its impacts: Summary of research and results from the ENSEMBLES project*, 166 pp., Met Off. Hadley Cent., Exeter U. K.

Von Storch, H., and F. Zwiers (2003), *Statistical Analysis in Climate Research*, 484 pp., Cambridge Univ. Press, Cambridge, U. K.

Wilson, P. S., and R. Toumi (2005), A fundamental probability distribution for heavy rainfall, *Geophys. Res. Lett.*, *32*, L14812, doi:10.1029/2005GL022465.

World Meteorological Organization (WMO) (2011), World Meteorological Organization provisional statement on the status of the global climate (2011), Geneva, Switzerland. [Available at http://www.wmo.int/pages/mediacentre/press_releases/gcs_2011_en.html].